Giant, Triply Resonant, Third-Order Nonlinear Susceptibility $\chi^{(3)}_{3\omega}$ in Coupled Quantum Wells

Carlo Sirtori, Federico Capasso, Deborah L. Sivco, and Alfred Y. Cho
AT&T Bell Laboratories, Murray Hill, New Jersey 07974
(Received 20 November 1991)

A new coupled-quantum-well semiconductor with triply resonant third-order nonlinear susceptibility $\chi^{(3)}_{3\omega}$ has been designed and demonstrated using AlInAs/GaInAs heterostructures grown by molecular-beam epitaxy. In order to maximize $|\chi^{(3)}_{3\omega}|$ our structure has been tailored in such a way to maximize the product of the dipole matrix elements of the relevant intersubband transitions while maintaining nearly equal spacing between the electronic bound states of the quantum wells. Experimental values of $|\chi^{(3)}_{3\omega}|$ as high as $\simeq 1\times10^{-14}$ (m/V)^2 at 10.7-μm pump wavelength have been obtained, in agreement with theoretical estimates.

PACS numbers: 78.20.−e

Band-structure engineering [1] has been advantageously used in recent years to artificially tailor the transport and optical properties of semiconductors, by exploiting the atomic-layer-thickness control and the large number of heterojunction combinations and doping profiles made possible by molecular-beam epitaxy (MBE) [2]. This approach can also be used to engineer new man-made semiconductors with very large nonlinear susceptibilities. For example, large second-order susceptibilities associated with mid-infrared intersubband transitions in asymmetric quantum wells have been recently reported by several groups [3–7].

In general, nonlinear susceptibilities $\chi^{(n)}$ associated with intersubband transitions within conduction-band quantum wells can be strongly enhanced, compared to susceptibilities of bulk semiconductors in the same wavelength range, using two effects. First, $\chi^{(n)}$ is proportional to the product of $n+1$ dipole matrix elements, each of which is typically 1 order of magnitude or more greater than bulk dipole matrix elements, since quantum-well sizes are typically much larger than atomic distances. Second, by tailoring well thicknesses and the shape of the wells, $\chi^{(n)}$ can be further enhanced using multiple resonances. In this work we have applied the above strategy to the design of new coupled-quantum-well semiconductors with extremely large $|\chi^{(3)}_{3\omega}|$ in the infrared ($\lambda\sim10$ μm). This has allowed us to observe for the first time intersubband third-harmonic generation (THG) in quantum wells. Previously Sa'ar *et al.* have reported the third-order intersubband optical Kerr effect, which is related to $\chi^{(3)}_{\omega,-\omega,\omega}$, in a rectangular, non-coupled-quantum-well structure [8]. Walrod *et al.* have demonstrated intersubband-nondegenerate four-wave mixing in AlGaAs/GaAs quantum wells [9].

To optimize $\chi^{(3)}_{3\omega}$ we have made use of the following expression (in MKS units), which is a good approximation for the triply resonant case [10]:

$$\chi^{(3)}_{3\omega}=\frac{e^4N}{\varepsilon_0}\frac{\langle z_{12}\rangle\langle z_{23}\rangle\langle z_{34}\rangle\langle z_{41}\rangle}{(\hbar\omega-\Delta E_{12}-i\Gamma_{12})(2\hbar\omega-\Delta E_{13}-i\Gamma_{13})(3\hbar\omega-\Delta E_{14}-i\Gamma_{14})}, \tag{1}$$

where N is the electron density in the wells, ε_0 the permittivity of the vacuum, e the electronic charge, $\Delta E_{ij}=E_j-E_i$ the energy separation between subbands j and i of the conduction-band quantum well, and Γ_{ij} and $\langle z_{ij}\rangle$ the half width at half maximum and the matrix element of the $i\rightarrow j$ intersubband transition, respectively. To maximize $|\chi^{(3)}_{3\omega}|$ one should look for a material where the relevant energy levels are equally spaced and where the product of the corresponding dipole matrix elements is maximum [see Eq. (1)]. It is hard to find a material with such characteristics [10,11]. Using appropriate combinations of quantum wells we have engineered a semiconductor structure which is an excellent approximation to the triply resonant situation described above (inset of Fig. 1). Note that using parabolic wells does not do the job. In an infinitely deep parabolic (or semiparabolic) well with negligible band nonparabolicities the energy levels are equally spaced and only the dipole matrix elements between adjacent states are nonzero; thus $\langle z_{14}\rangle=0$ so that $\chi^{(3)}=0$. For compositionally graded parabolic or semiparabolic wells of finite depth the deviation from the ideal harmonic-oscillator potential caused by the finite well depth and band nonparabolicities gives rise to $\langle z_{14}\rangle\neq0$. Nevertheless, $\langle z_{14}\rangle$ is always $\ll\langle z_{12}\rangle,\langle z_{23}\rangle,\langle z_{34}\rangle$ and typically does not exceed 1 Å for an energy-level separation ≈120 meV in AlGaAs parabolic wells [12]. For the AlInAs/GaInAs structure of Fig. 1, instead, all the relevant matrix elements are large: $\langle z_{41}\rangle=8.6$, $\langle z_{12}\rangle=13$, $\langle z_{23}\rangle=22.7$, and $\langle z_{34}\rangle=22.6$ Å. The calculated energy levels are $E_1=151$, $E_2=270$, $E_3=386$, and $E_4=506$ meV [13].

Our AlInAs/GaInAs structure, grown by MBE and lattice matched to a semi-insulating (100) InP substrate, consists of forty coupled-well periods (Fig. 1) separated by 150-Å undoped AlInAs barriers. Only the thickest well is n-type doped (nominally $=1\times10^{18}$ cm^{-3}). The multi-quantum-well region is separated from n^+ 4000-

 © 1992 The American Physical Society

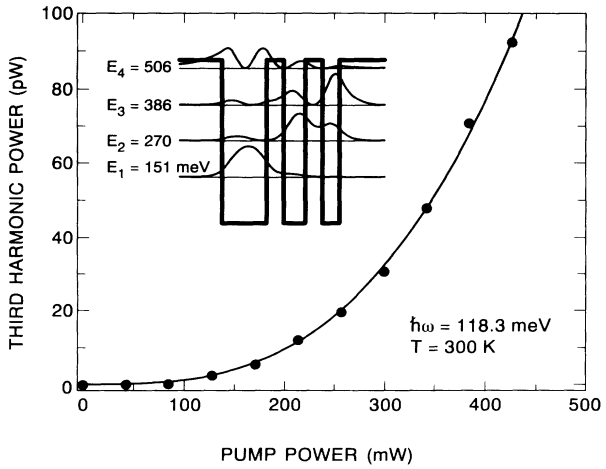

FIG. 1. Third-harmonic generation as a function of pump power. The solid curve represents the fit with a cubic to the data and demonstrates that the third-harmonic signal increases with the cube of the pump power. The pump is linearly polarized in such a way to maximize the component of the electric field normal to the layers. Inset: The energy-band diagram of a single period of the AlInAs/GaInAs coupled-quantum-well structure. The GaInAs wells have thicknesses of 42, 20, and 18 Å, respectively, and are separated by 16-Å AlInAs barriers. Shown are the positions of the calculated energy subbands and the corresponding modulus squared of the wave functions.

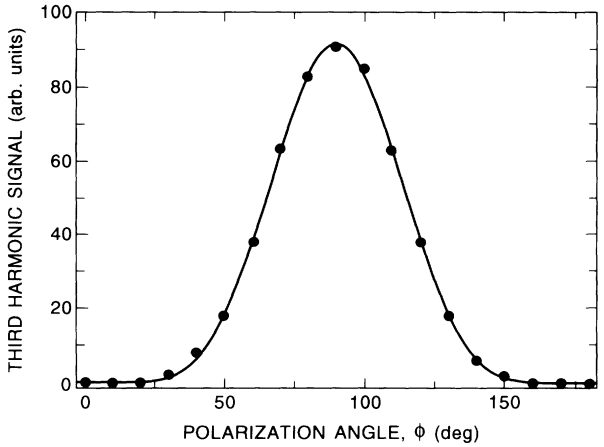

FIG. 2. Third-harmonic power as a function of pump polarization. The data follow the expected $\sin^6\phi$ dependence (solid curve).

Å-thick GaInAs cladding layers by 150-Å undoped AlInAs barriers. Transmission measurements with a Fourier transform interferometer (FTIR) using a multipass waveguide geometry [6] at 300 K found three absorbance peaks at energies $\Delta E_{12}=102$, $\Delta E_{13}=232$, and $\Delta E_{14}=344$ meV. The small differences between these values and the ones calculated for the optimized structure (Fig. 1) are due to small variations between the nominal and measured layer thicknesses [14]. From the areas under the absorbance peaks, fitted with a Lorentzian line shape, the electron sheet density in the well can be estimated using the calculated dipole matrix elements. We found $n_s=(3.5\pm1)\times10^{11}$ cm^{-2}, in reasonable agreement with the nominal doping concentration.

For the experiments the samples were cleaved in narrow strips and the cleaved edges were polished at 45° to provide a two-pass waveguide. In this geometry the CO_2-pump-laser beam, after entering the sample at normal incidence (on one of the polished edges) and traversing the coupled-well region, is reflected off the top surface and passes a second time through the multilayers. For the experiment we used a highly stable cw CO_2 laser. A $\lambda/4$ plate converts the radiation into circularly polarized light which is then chopped at 2 kHz. After passing through a telescope to reduce its divergence, the beam traverses two high-extinction polarizers. By appropriately varying the angle between the axes of the latter, one can vary the power and the linear polarization of the incident light. A lens focuses the light normal to one of the 45° edges of the sample. The third-harmonic radiation ($\lambda\simeq3.5$ μm) is collected by a lens, followed by a sapphire window to cut the pump beam, an analyzer, and a short-pass ($\lambda_c=4.1$ μm) filter. The signal is detected with a calibrated N_2-cooled InSb detector.

The third-harmonic power is expected to increase with the third power of the pump beam [9]. In addition, only the component normal to the layers of the electric field of the incident pump wave contributes to intersubband THG. Thus if $\phi=90°$ represents the orientation of the polarization of the incident pump beam, which maximizes the component of the electric field normal to the layers, rotating the polarization of the pump will reduce the third-harmonic power according to $\sin^6\phi$. The measured third-harmonic power (Figs. 1 and 2) verifies the above dependence on pump power and polarization angle. We also verified that the third-harmonic radiation is linearly polarized in the plane defined by the propagation direction and the normal to the layers, as expected from the polarization selection rules of intersubband transitions.

To derive the expression for the third-harmonic power generated in our structure, we observe that the distance traveled by the pump and third-harmonic beam in each of the two passes through the superlattice is much smaller than the coherence length ($l_c=28$ μm at $\lambda=10.6$ μm). In addition, the phase mismatch acquired by the fundamental and third-harmonic waves in the top InGaAs cladding layer, between the two passes through the superlattice, is negligible since the distance traveled in this region (≈1.1 μm) is $\ll l_c$ and the relative phase shift upon reflection from the top surface is negligible due to the near equality of the refractive indexes at 3ω and ω. The expression for $P(3\omega)$ can then be simply derived from Maxwell's equations including the absorption losses at ω and 3ω, for the case of phase matching and no pump de-

pletion [15],

$$P(3\omega)=\frac{3}{4}\frac{\mu_0^2\omega^2}{n_\omega^3 n_{3\omega}}\frac{\sin^8\theta}{S^2}\exp\left[-\left(\frac{3}{2}\alpha_\omega+\frac{1}{2}\alpha_{3\omega}\right)L\right]\times\left[\frac{\sinh(\alpha L/2)}{\alpha/2}\right]^2|\chi_{3\omega}^{(3)}|^2P^3(\omega)\,, \quad (2)$$

where $P(\omega)$ is the pump power (i.e., the incident power minus the reflected power), S is the area of the laser spot (diameter=42 μm), n_ω and $n_{3\omega}$ are the refractive indices at ω and 3ω, α_ω and $\alpha_{3\omega}$ are the absorption coefficients for the pump and third harmonic, respectively (obtained from the FTIR data), $\alpha=\frac{3}{2}\alpha_\omega-\frac{1}{2}\alpha_{3\omega}$, θ is the angle of incidence with respect to the normal to the plane of the layers (45° in our case), L is the interaction length, which for our double-pass structure reduces to 2(active layer thickness)/cosθ, and μ_0 is the vacuum permittivity. In deriving Eq. (2) we have considered the case of a pump linearly polarized so that the component of the electric field normal to the layers is maximized. Since this component is proportional to sinθ, the contribution of the pump power to THG comes in as $[P(\omega)\sin^2\theta]^3$ in Eq. (2). The additional $\sin^2\theta$ factor in Eq. (2) is a result of the transformation from the crystal coordinate system to the laboratory frame used to describe the field propagation.

By best-fitting the data of Fig. 1, and using Eq. (2), one obtains $|\chi_{3\omega}^{(3)}|=0.6\times10^{-14}$ (m/V)^2.

The dependence of THG on pump wavelength was also investigated. The data are shown in Fig. 3(a). The power increases rapidly as the photon energy approaches 115 meV, corresponding to the resonance condition

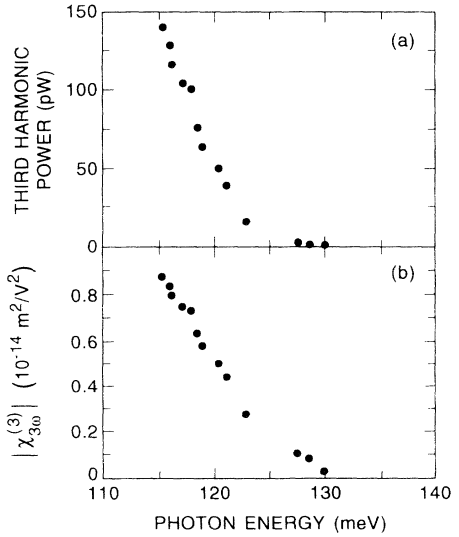

FIG. 3. (a) Third-harmonic power and (b) third-order susceptibility $|\chi_{3\omega}^{(3)}|$ as a function of pump photon energy. The pump power is 300 mW.

$3\hbar\omega=E_4-E_1$. The range of photon energies is limited by the CO_2 laser. Note that peaks corresponding to $\hbar\omega=\Delta E_{21}$ and $2\hbar\omega=\Delta E_{31}$ cannot be resolved since the energy differences between ΔE_{12}, ΔE_{23}, and ΔE_{34} are less than the broadening. From the data of Fig. 3(a) and substituting in Eq. (2) the experimental values of all the quantities involved, one obtains $|\chi_{3\omega}^{(3)}|$ as a function of $\hbar\omega$ [Fig. 3(b)]. Using the calculated $\langle z_{ij}\rangle$ in Eq. (1) and the half widths at half maximum of the FTIR absorbance peaks ($\Gamma_{12}=20$, $\Gamma_{13}=16$, and $\Gamma_{14}=18$ meV) as an estimate of the broadenings Γ_{ij} in Eq. (1), one obtains $|\chi_{3\omega}^{(3)}|\simeq1.3\times10^{-14}$ (m/V)^2 at $\hbar\omega=115$ meV, which compares favorably with the experimental value, i.e., 0.9×10^{-14} (m/V)^2 (Fig. 3). To our knowledge this is the largest third-order nonlinear susceptibility reported in any material. It is about 5 orders of magnitude greater than $|\chi_{3\omega}^{(3)}|$ associated with bound electrons in InAs and GaAs [16], at comparable wavelengths. The value reported by Sa'ar *et al.* [8] for $\chi_{\omega,-\omega,\omega}^{(3)}$ at $\lambda\approx10.6$ μm in a GaAs/AlGaAs multiwell structure is 1.7×10^{-15} (m/V)^2. The measured peak value of $|\chi_{3\omega}^{(3)}|$ is limited, in our present structure, by the broadening Γ_{ij} of the intersubband transitions. The latter is primarily determined by in-plane layer-thickness fluctuations. By varying growth conditions (e.g., using interrupted growth) one might be able to reduce the broadening. If this can be achieved, the small conversion efficiency of our structure could be greatly enhanced by suitably detuning the pump photon from resonance, while preserving the two- and three-photon resonance condition (this will be satisfied, in the present design, at $\hbar\omega=115$ meV, provided the broadening Γ_{ij} can be reduced) to reduce absorption losses, and by modifying the sample geometry in order to increase the interaction length. A similar strategy has been successfully used recently to optimize intersubband second-harmonic generation in asymmetric stepped quantum-well structures [17].

It is interesting to note that THG can also arise in our structure from frequency mixing between the second-harmonic and pump waves. From our previous measurements of $|\chi_{2\omega}^{(2)}|$ in coupled-quantum-well AlInAs/GaInAs structures [6,7] and the amount of second-harmonic power generated in our structure [$\sim$1 nW for $P(\omega)$ =200 mW], one can easily estimate that the third-harmonic power generated by this mechanism does not exceed a few tenths of a picowatt.

In conclusion, we have reported a new quantum-well structure which exhibits an extremely large third-order susceptibility associated with THG. Using band-structure engineering a large variety of new structures can be created, which are expected to exhibit a rich variety of nonlinear optical effects with large susceptibilities. Particularly intriguing in this respect is the possibility of field tuning the latter, since the wave functions and energy levels can be easily controlled in quantum wells by the application of small voltages. This was recently demonstrated

by us in the case of second-harmonic generation, by resonantly tuning $\chi^{(2)}_{2\omega}$ via the Stark effect [7].

It is a pleasure to acknowledge useful conversations with B. F. Levine, C. G. Bethea, and M. Mastrapasqua. C.S. acknowledges financial support from Technobiochip, Marciana, Italy.

[1] For recent reviews, see F. Capasso, MRS Bull. **16**, 23 (1991); F. Capasso and S. Datta, Phys. Today **43**, No. 2, 74 (1990), and references therein.

[2] A. Y. Cho, J. Cryst. Growth **111**, 1 (1991), and references therein.

[3] M. M. Fejer, J. J. B. Yoo, R. L. Byer, A. Harwit, and J. S. Harris, Jr., Phys. Rev. Lett. **62**, 1041 (1989).

[4] P. Boucaud, F. H. Julien, D. D. Yang, J. M. Lourtioz, E. Rosencher, P. Bois, and J. Nagle, Appl. Phys. Lett. **57**, 215 (1990).

[5] E. Rosencher, P. Bois, J. Nagle, E. Costard, and S. Delaitre, Appl. Phys. Lett. **56**, 1822 (1990).

[6] C. Sirtori, F. Capasso, D. L. Sivco, S. N. G. Chu, and A. Y. Cho, Appl. Phys. Lett. **59**, 2302 (1991).

[7] C. Sirtori, F. Capasso, D. L. Sivco, A. L. Hutchinson, and A. Y. Cho, Appl. Phys. Lett. (to be published).

[8] A. Sa'ar, N. Kuze, J. Feng, I. Grave, and A. Yariv, in Proceedings of NATO Advanced Research Workshop on Intersubband Transitions in Quantum Wells, Cargese, France, 1991 (Pergamon, New York, to be published).

[9] D. Walrod, S. Y. Auyang, P. A. Wolff, and M. Sugimoto, Appl. Phys. Lett. **59**, 2932 (1991).

[10] Y. R. Shen, *The Principles of Nonlinear Optics* (Wiley, New York, 1984). Note that in our structure the local-field correction can be shown to be negligible since we are dealing with a diluted system (Fermi gas of electrons) with a density many orders of magnitude smaller than in solids where such corrections are important.

[11] Although resonant effects in THG have been reported in several atomic and molecular vapors (see Ref. [9]), to the best of our knowledge, ours is the first experimental report of the triply resonant case.

[12] In a recent paper on far-infrared ionization of semiparabolic quantum wells [W. W. Bewley, C. L. Felix, J. J. Plombon, B. Galdrikian, M. S. Sherwin, M. Sundaram, A. C. Gossard, and B. Birnir (to be published)] the authors have briefly discussed the observation of THG. However, no data demonstrating that this effect is related to $\chi^{(3)}_{3\omega}$ have been presented. Our calculations show that in their wide parabolic wells (2400 Å), $\langle z_{14}\rangle \ll 1$ Å, so that the resulting $|\chi^{(3)}_{3\omega}|$ should be very small.

[13] For the AlInAs/GaInAs parameters we used $\Delta E_c = 0.53$ eV, $m_c^* = 0.043 m_0$; the nonparabolicity coefficient $\gamma = 1.03 \times 10^{-18}$ m^2. The wave functions were calculated in the envelope function approximation following G. Bastard, Phys. Rev. B **24**, 5693 (1981). Nonparabolicities were taken into account using the method of D. F. Nelson, R. C. Miller, and D. A. Kleinman, Phys. Rev. B **35**, 7770 (1987).

[14] Transmission electron microscopy measurements give the following values for the layer thicknesses (from left to right in the inset of Fig. 1): 45 Å (GaInAs), 15 Å (AlInAs), 22 Å (GaInAs), 13 Å (AlInAs), 20 Å (GaInAs).

[15] Equation (2) is a generalization, for the phase-matched case, of a formula given by S. Singh, in *CRC Handbook of Laser Science and Technology: Optical Materials —Nonlinear Optical Properties-Radiation Damage,* edited by Marvin Webber (CRC, Boca Raton, 1986), Vol. III.

[16] W. K. Burns and N. Bloembergen, Phys. Rev. B **4**, 3437 (1971).

[17] F. H. Julien, in Ref. [8].